Supplementary figures

Siah2-GRP78 interaction regulates ROS and provides a proliferative advantage to *Helicobacter pylori*-infected gastric epithelial cancer cells

Pragyesh Dixit[1], Swathi Shivaram Suratkal[1,#], Shrikant Babanrao Kokate[1,$], Debashish Chakraborty[1], Indrajit Poirah[1], Supriya Samal[1], Niranjan Rout[2], Shivaram P. Singh[3], Arup Sarkar[4], Asima Bhattacharyya[1,*]

Affiliations:[1]School of Biological Sciences, National Institute of Science Education and Research (NISER) Bhubaneswar, An OCC of Homi Bhabha National Institute, P.O. Bhimpur-Padanpur, Via Jatni, Dist. Khurda, Jatni 752050, Odisha, India; [2]Department of Pathology, Acharya Harihar Post Graduate Institute of Cancer, Cuttack 753007, Odisha, India; [3]Department of Gastroenterology, SCB Medical College, Cuttack 753007, Odisha, India; [4]Trident Academy of Creative Technology, Bhubaneswar 751024, Odisha, India.

Current address: [#]Program in Neuroscience and Behavioral Disorders, Duke-NUS Medical School, 8 College Road, Singapore 169857, Singapore.

[$]HiLIFE Institute of Biotechnology, University of Helsinki, P.O. Box 56, 00014, Helsinki, Finland.

Correspondence: *School of Biological Sciences, National Institute of Science Education and Research (NISER), An OCC of Homi Bhabha National Institute, P.O. Bhimpur-Padanpur, Via Jatni, Dist. Khurda 752050, Odisha, India. Tel: +91-674-2494210, e-mail: asima@niser.ac.in

A

Description	Score	Coverage	# Unique Peptides	Predicted MW [kDa]
78 kDa glucose-regulated protein OS=Homo sapiens GN=HSPA5 PE=1 SV=2 - [GRP78_HUMAN]	1182.81	42.66	21	72.3
Heat shock 70 kDa protein 1-like OS=Homo sapiens GN=HSPA1L PE=1 SV=2 - [HS71L_HUMAN]	343.09	11.08	1	70.3
Heat shock protein HSP 90-beta OS=Homo sapiens GN=HSP90AB1 PE=1 SV=4 - [HS90B_HUMAN]	341.00	17.68	5	83.2
Stress-70 protein, mitochondrial OS=Homo sapiens GN=HSPA9 PE=1 SV=2 - [GRP75_HUMAN]	216.89	18.70	9	73.6
Heat shock protein HSP 90-alpha OS=Homo sapiens GN=HSP90AA1 PE=1 SV=5 - [HS90A_HUMAN]	195.47	9.97	1	84.6
Protein disulfide-isomerase A4 OS=Homo sapiens GN=PDIA4 PE=1 SV=2 - [PDIA4_HUMAN]	178.91	21.40	10	72.9
6-phosphofructokinase type C OS=Homo sapiens GN=PFKP PE=1 SV=2 - [K6PP_HUMAN]	67.68	9.82	4	85.5
Far upstream element-binding protein 2 OS=Homo sapiens GN=KHSRP PE=1 SV=4 - [FUBP2_HUMAN]	57.31	5.20	3	73.1
Threonine--tRNA ligase, cytoplasmic OS=Homo sapiens GN=TARS PE=2 SV=1 - [E7ERI3_HUMAN]	51.40	3.65	2	70.3
Ral guanine nucleotide dissociation stimulator-like 1 OS=Homo sapiens GN=RGL1 PE=2 SV=1 - [F5H6U6_HUMAN]	40.13	1.62	1	83.5
6-phosphofructokinase, liver type OS=Homo sapiens GN=PFKL PE=1 SV=6 - [K6PL_HUMAN]	36.33	4.36	1	85.0
X-ray repair cross-complementing protein 5 OS=Homo sapiens GN=XRCC5 PE=1 SV=3 - [XRCC5_HUMAN]	36.08	4.10	2	82.7
Junction plakoglobin OS=Homo sapiens GN=JUP PE=1 SV=3 - [PLAK_HUMAN]	22.78	7.92	4	81.7
RNA polymerase II elongation factor ELL2 OS=Homo sapiens GN=ELL2 PE=1 SV=2 - [ELL2_HUMAN]	22.68	1.88	1	72.3
Glycine--tRNA ligase OS=Homo sapiens GN=GARS PE=1 SV=3 - [SYG_HUMAN]	0.00	1.49	1	83.1

B

MKLSLVAAMLLLLSAARAEEEDKKEDVGTVVGIDLGTTYSCVGVFKNGRVEIIANDQGNRITPSYVAFTPEGERLIG
DAAKNQLTSNPENTVFDAKRLIGRTWNDPSVQQDIKFLPFKVVEKKTKPYIQVDIGGGQTKTFAPEEISAMVLTKM
KETAEAYLGKKVTHAVVTVPAYFNDAQRQATKDAGTIAGLNVMRIINEPTAAAIAYGLDKREGEKNILVFDLGGGT
FDVSLLTIDNGVFEVVATNGDTHLGGEDFDQRVMEHFIKLYKKKTGKDVRKDNRAVQKLRREVEKAKRALSSQH
QARIEIESFYEGEDFSETLTRAKFEELNMDLFRSTMKPVQKVLEDSDLKKSDIDEIVLVGGSTRIPKIQQLVKEFFNG
KEPSRGINPDEAVAYGAAVQAGVLSGDQDTGDLVLLDVCPLTLGIETVGGVMTKLIPRNTVVPTKKSQIFSTASDN
QPTVTIKVYEGERPLTKDNHLLGTFDLTGIPPAPRGVPQIEVTFEIDVNGILRVTAEDKGTGNKNKITITNDQNRLTPE
EIERMVNDAEKFAEEDKKLKERIDTRNELESYAYSLKNQIGDKEKLGGKLSSEDKETMEKAVEEKIEWLESHQDA
DIEDFKAKKKELEEIVQPIISKLYGSAGPPPTGEEDTAEKDEL

C

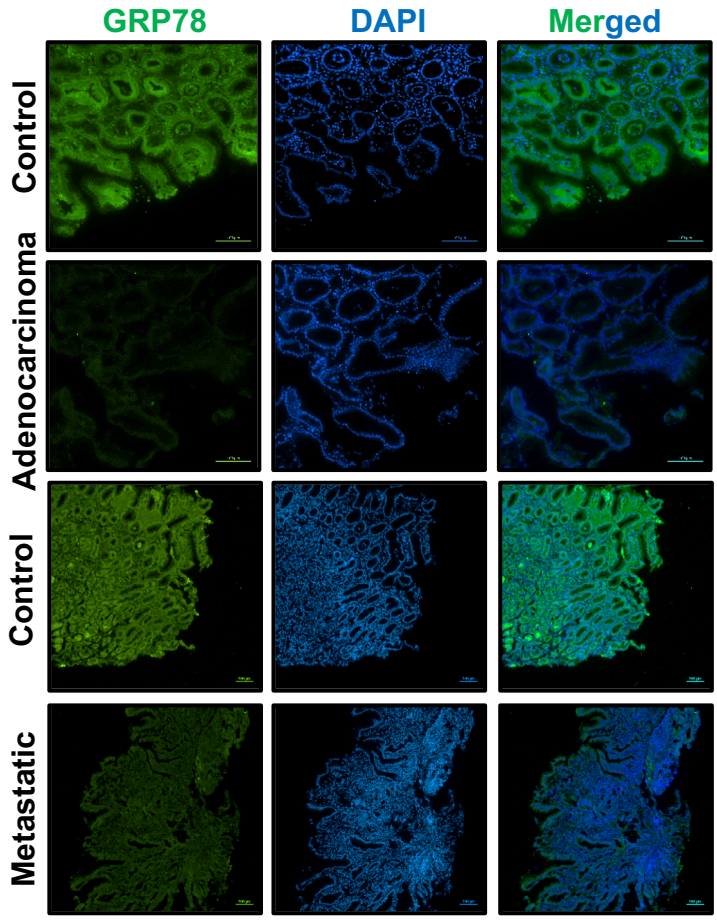

Fig. S1 Mass spectrometry (MS) result and histological expression of GRP78 protein. **A** Table showing MS results for GRP78 along with other proteins. **B** The amino acid sequence of GRP78 depicting the presence of partial (VXP) and full Siah-degron motif (PXXXVXP) (underlined). **C** Human antral adenocarcinoma and metastatic GC biopsy tissues showing the status of GRP78 protein. Scale bars=100 μm.

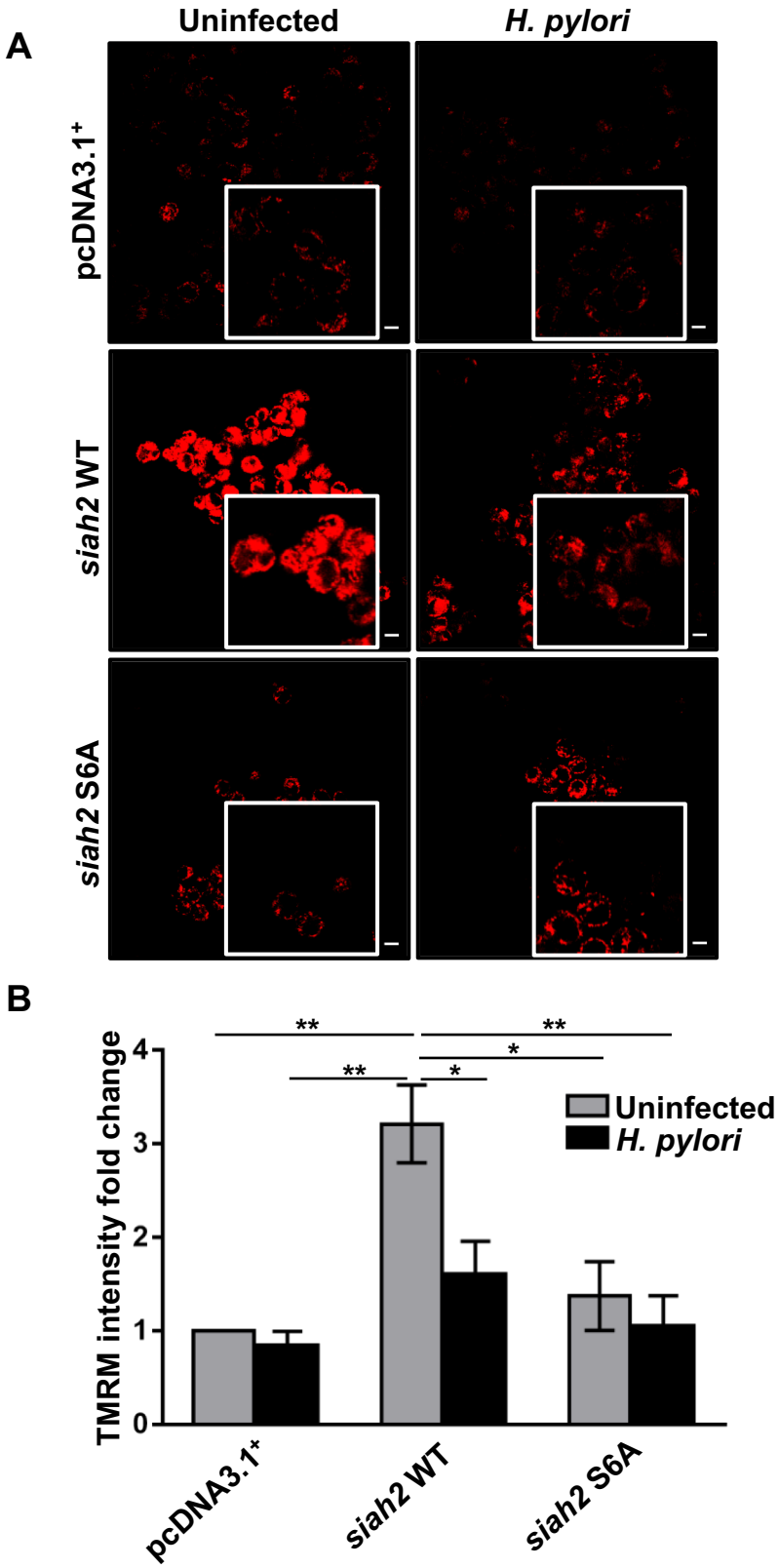

Fig. S2 Siah2 phospho-null mutant S6A disrupts mitochondrial membrane potential as depicted by reduced TMRM intensity **A** Confocal micrographs showing intensity of TMRM loaded uninfected or infected pcDNA3.1+, *siah2* WT and *siah2* S6A stably-expressing MKN45 cells. Scale bars=10 μm. **B** Graphical representation of TMRM intensity. Statistical significance determined by two-way ANOVA followed by Tukey's post hoc analysis. n=3. Graphs represent mean ± sem. *P < 0.05, **P < 0.01.

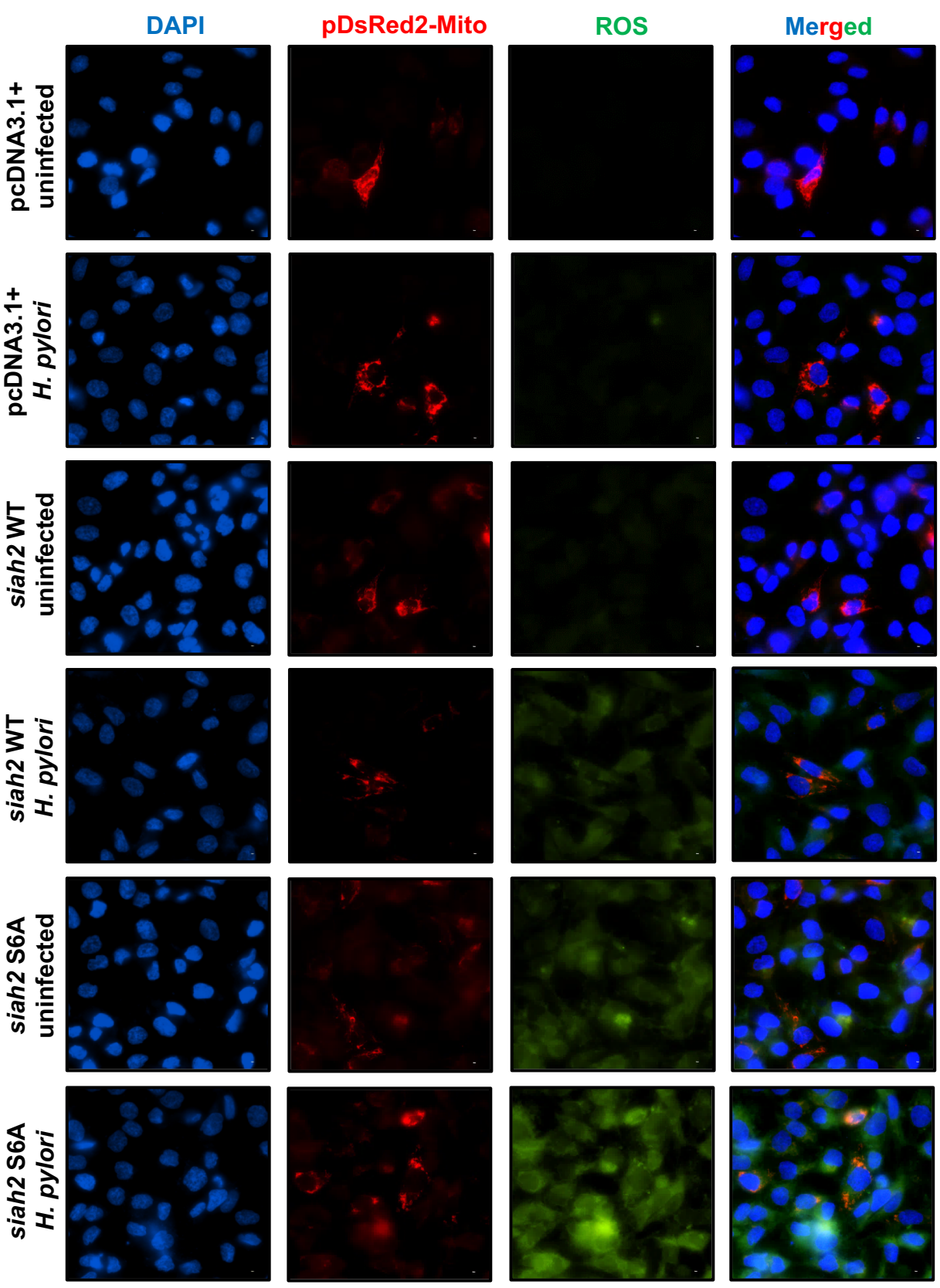

Fig. S3 *H. pylori*-mediated Siah2 phosphorylation regulates cellular and mitochondrial ROS. Confocal micrographs from uninfected or infected pcDNA3.1+, *siah2* WT and *siah2* S6A overexpression plasmid transiently-transfected pDsRed2-Mito stably-expressing AGS cells depicting ROS level. Scale bars represent 10 μm.

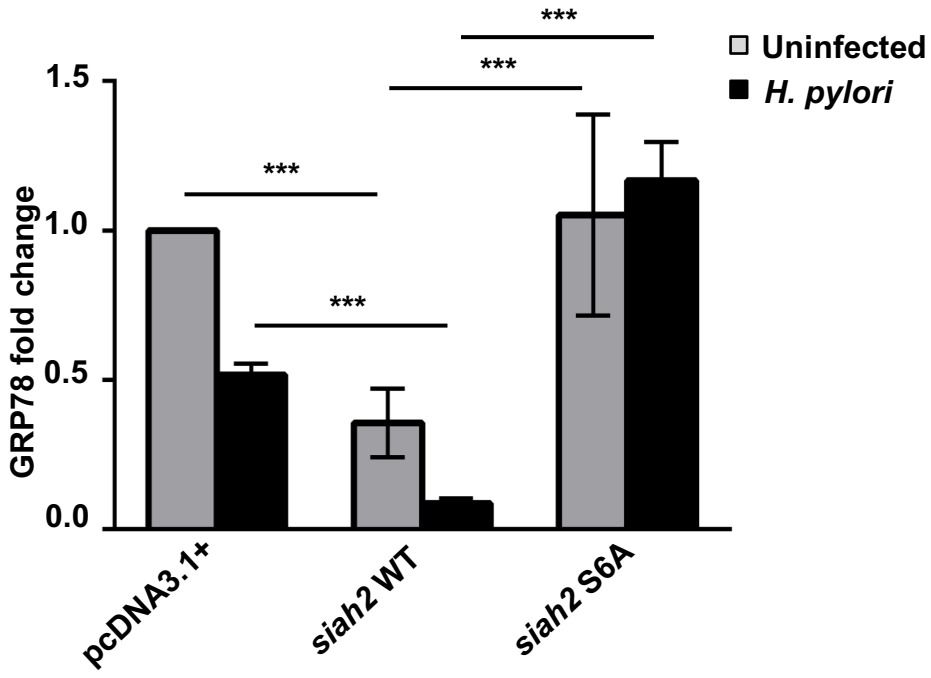

Fig. S4 Secretion of GRP78 is regulated by *H. pylor*i-mediated Siah2 phosphorylation. Graphical representation of the fold change in the secreted GRP78 as detected by ELISA. Statistical significance is determined by two-way ANOVA followed by Tukey's post hoc analysis. n = 3. Graphs represent mean ± sem. ***$P < 0.001$.

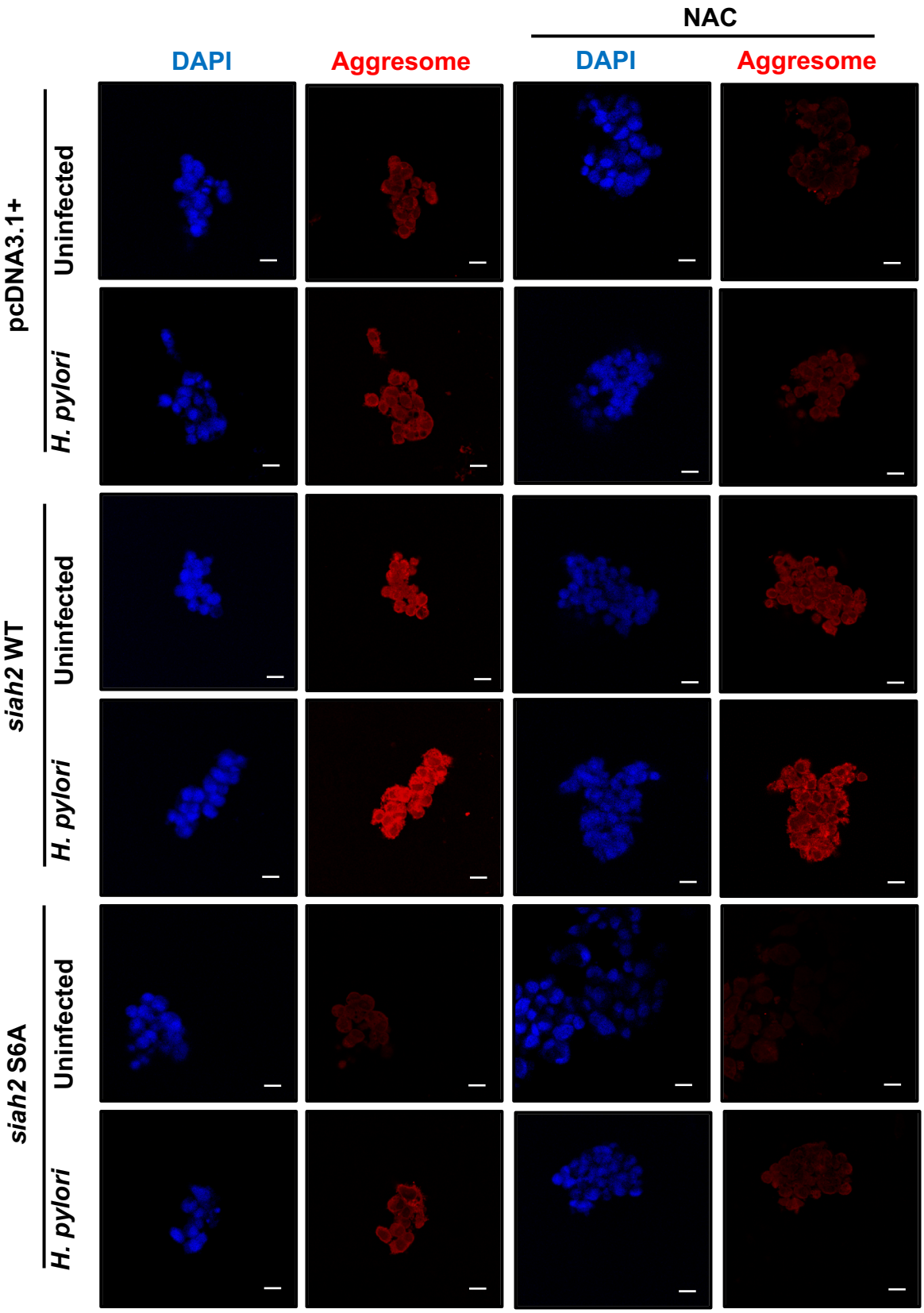

Fig. S5 Aggresome formation is Siah2 and ROS-dependent in *H. pylori*-infected GECs. Confocal microscopy images showing the status of aggresome formation in uninfected or infected NAC-treated pcDNA3.1+, *siah2* WT and *siah2* S6A MKN45 stable cells. Scale bars = 10 μm.

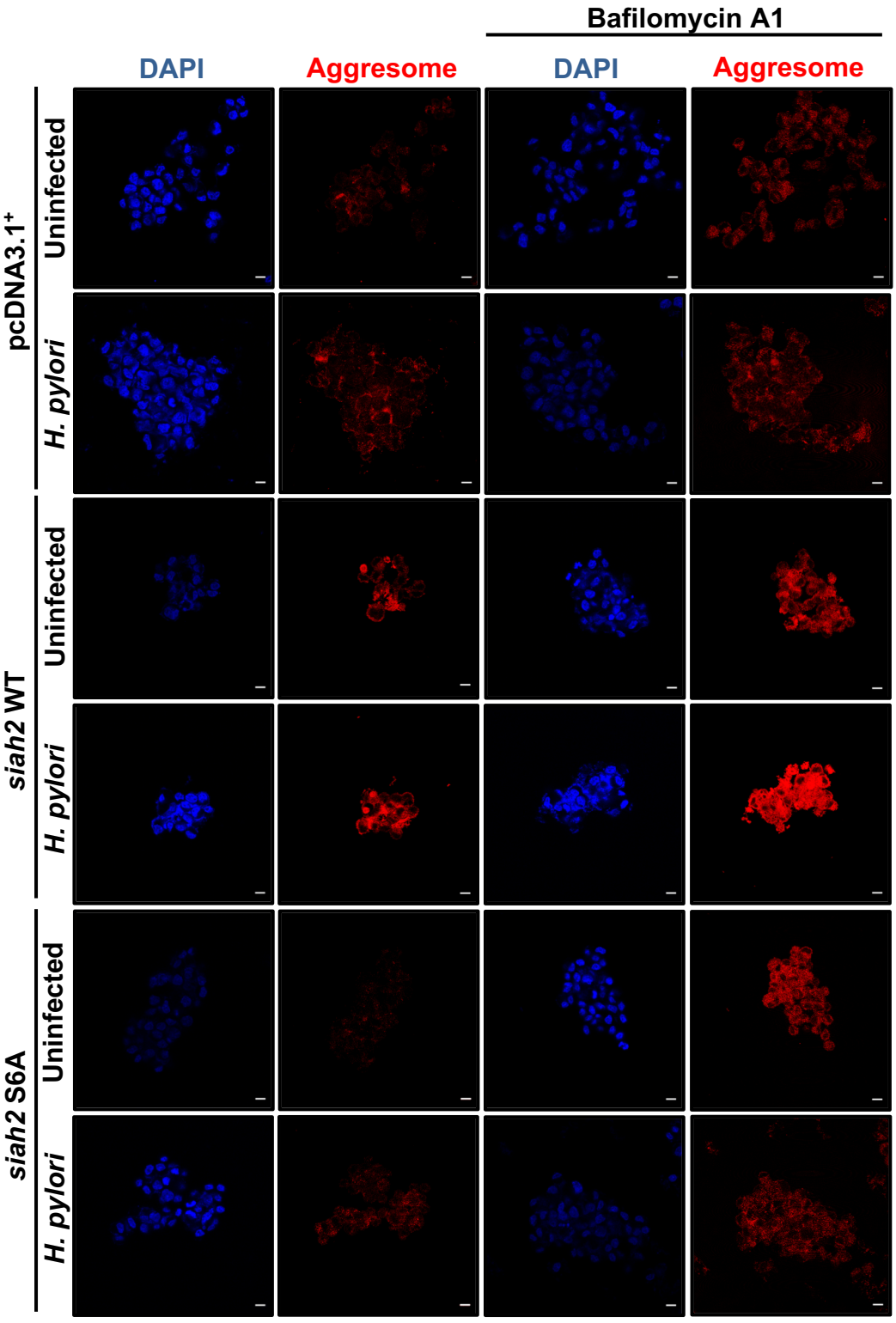

Fig. S6 Aggresome formation is Siah2-dependent reciprocally correlated with autophagy in *H. pylori*-infected GECs. Confocal microscopy images showing the status of aggresome formation in uninfected or infected bafilomycin A1-treated pcDNA3.1+, *siah2* WT and *siah2* S6A MKN45 stable cells. Scale bars = 10 μm.